Mechanistic-empirical Design of Perpetual Road Pavement Using Strain-based Design Approach

Manoj Kumar Sahis[1*], Partha Pratim Biswas[1], Sanjib Sadhukhan[1], Geetam Saha[1]

[1] Department of Construction Engineering, Faculty of Engineering & Technology, Jadavpur University, 188, Raja S.C. Mallick Rd, Kolkata - 700032, West Bengal
[*] Corresponding author, e-mail: manojkumar.sahis@jadavpuruniversity.in

Abstract

Present paper deals with the development of a Mechanistic-Empirical model of the strain-based design of perpetual road pavement using Odemark's principle. The bituminous pavement which can withstand minimum design traffic of 300 msa has been classified as perpetual pavement in this paper. The pavement has been considered as a three-layered system with a top layer of bituminous mix followed by unbound granular materials which rest on soil subgrade. The constituent bituminous layer thickness in the pavement has been determined by limiting the radial tensile strain at the bottom of the bituminous layer against fatigue and the vertical compressive strain at the top of the subgrade against rutting. The allowable strain against rutting and fatigue has been used in the present analysis from mechanistic-empirical correlations recommended in IRC:37-2018. The pavement section has been transformed into a homogeneous system by Odemark's method for application of Boussinesq's theory. To validate the thickness of the perpetual pavement, the strain at different layer interfaces in the pavement was compared using IITPAVE software, which shows the pavement section using present method is safe against rutting but marginally fails under fatigue. Moreover, conventional pavement thickness obtained using IRC:37-2018 were compared with the present method, which shows reasonably good convergence. It has been found that the bituminous layer thickness in a layered system of pavement seems to be more sensitive to fatigue than rutting. In this backdrop, modified fatigue and rutting strain values have been recommended for the design of perpetual road pavement.

Keywords

bituminous layer, fatigue, rutting, granular layer, perpetual pavement, Odemark

1 Introduction

The unbridled increment of traffic volumes and unexpected axle loads along with the gradual demands for freight corridor has impelled to conceptualize the perpetual pavement. Presently, flexible pavement is generally designed considering the structure of the pavement as a multilayered system. The basic method of flexible pavement design started with an assumption of a two-layered system and gradually evolved into a multi-layered system of pavement design. The design of pavement primarily depends on the methodology adopted and the boundary conditions assumed in course of design. The main concept of perpetual pavements is that the asphalt pavement should be constructed with an impermeable, rut- and wear-resistant top layer placed on a rut-resistant and durable intermediate layer with a fatigue-resistant and durable base layer. Limiting strain distribution and maximum fatigue ratios to resist bottom-up FC (fatigue cracking) is sometimes used to design a perpetual pavement [1]. Although various endurance limits of perpetual pavement have been proposed, none have been determined and field validated for efficient design [2–6]. The National Center for Asphalt Technology (NCAT) suggested the FEL (Fatigue Endurance Limit) [5, 7–10, 12] alue for most perpetual pavement designs is in the range of 70 to 100 με. This concept was first proposed by Monismith and McLean based on the laboratory test [11]. However, based on the results of different in-service pavement sections, some researchers suggested the Fatigue Resistance Layer (FRL) [8, 13] can withstand up to 150 με depending on the type of bituminous mixture used [14–16]. Lee et al. [17] reported the cost-effective PP (perpetual pavement) design alternatives to improve design optimization, material quality, and constructability. The structural and economic validations indicated that the design alternatives analytically meet expected performance limits, which

last for the 50-year design life without significant structural failures, with a total agency cost saving of up to 19% compared with the current design procedure. Priyanka et al. [18] proposed two polymer-modified Superpave mixtures for intermediate and base layers, based on laboratory experiments after judging the parameters like moisture susceptibility, rutting resistance, fatigue behavior, and resilient modulus. The critical fatigue and rutting strains of perpetual pavements were found to be within the limits when evaluated with KENPAVE. The study proposed that Superpave mixtures can be used as an alternative for conventional pavements.

Qadir et al. [19] investigated and compared the performance of polymer-modified asphalt (PMA), polypropylene (PP)-fiber-modified, and neat asphalt mixes, on their rutting behavior and life cycle costs. The study suggested that although the initial cost of other mixes is higher with respect to conventional asphalt mix. But considering the life cycle cost, the PMA mixes can be a better choice to limit rutting on the pavement. Moreover, a linear regression model was developed to depict the rutting behavior with temperature and polymer type. Islam et al. [20] studied the validity of the assumptions related to the design of perpetual pavement sections using PerRoad and AASHTOWare Pavement ME Design software. Moreover, by using the bottom-up cracking and FWD deflection data, fatigue life and Layer moduli were estimated. The comparative results as derived from PerRoad showed a higher value than AASHTOWare Pavement ME design values. The study also recommended that the rich bituminous mix if used in the base layer can be useful as the most successful perpetual pavement. Kollaros et al. [21] proposed a methodology to reduce the maintenance cost of perpetual asphalt pavements by reduction of damage per million equivalent single axle loads and increase in expected service-life has been achieved with the increase of moduli values and thicknesses of different layers in the pavement structure.

Scheer [22] evaluated the performance of perpetual pavement structures through the installation of several sensors in a different layer in a pavement. Pavement response thus obtained as fatigue strain at a critical location in pavement section was compared with expected strain to assess the durability of pavement.

The influence of axle configuration, speed, and tire pressure were analyzed to understand its effects on pavement responses. Das [23] presented review on various pavement design guidelines on the structural design of asphalt pavements with reference to the design principles employed. The focus was primarily kept on the mechanistic-empirical pavement design approach. The discussion covers a few specific aspects of asphalt pavement design. Mazumder et al. [24] reviewed the importance of perpetual pavement in future road networks and also mentioned the mechanistic-empirical design principles and differences with conventional pavement. Liao and Sargand [25] presented a three-dimensional linear viscoelastic finite element model to simulate the behavior of a perpetual pavement structure subjected to traffic loading at different temperatures and vehicular speeds. Romanoschi et al. [26] investigated the suitability of the perpetual pavements concept for Kansas highway pavements by constructing four thick flexible pavements. A detailed instrumented mechanism was employed to find the permissible strain limit, which showed the developed strain remains well within the endurance limit even in hot summer. Timm et al. [16] proposed a design procedure (PerRoad) based on principles of perpetual pavement. Moreover, the study also focused on developing a Monte Carlo simulation-based reliability approach to minimize the risk of structural failure.

2 Objective of the study
The following are the objectives that may be achieved from the present analytical study.
1. To develop a strain-based model of perpetual pavement design based on a method of an equivalent thickness (MET) using fatigue and rutting as design criteria.
2. To validate the results obtained using the present methodology with another strain-based analytical approach.

3 Perpetual Pavement Design Model based on fatigue and rutting criteria
In this paper, the pavement system has been characterized as a three-layer system as shown in Fig. 1. The top layer consists of a bituminous binder course with thickness h_1 and resilient modulus E_1. The middle layer consists of unbound granular materials with thickness h_2 and composite elastic modulus of E_2 which ultimately rests on soil subgrade with an elastic modulus of E_3. The subgrade layer in a three-layered system has been considered as the foundation of pavement crust. In this paper, the elastic modulus of the unbound granular layer has been estimated using Eq. (1) as recommended by Powell et al. [27].

$$E_2 \left(MPa \right) = 0.2 \times \left(h_2 \right)^{0.45} \times E_3 , \tag{1}$$

where h_2 = thickness of the unbound granular layer, which is the summation of granular base and sub-base thickness (mm).

In this paper, the pavement system has been characterized as a three-layer system as shown in Fig. 1.

The top layer consists of a bituminous binder course with thickness h1 and resilient modulus E_1. The middle layer consists of unbound granular materials with thickness h_2 and composite elastic modulus of E_2 which ultimately rests on soil subgrade with an elastic modulus of E_3. The subgrade layer in a three-layered system has been considered as the foundation of pavement crust. In this paper, the elastic modulus of the unbound granular layer has been estimated using Eq. (1) as recommended by Powell et al. [28].

$$E_3\left(MPa\right)=10\times CBR \ for \ CBR \leq 5\% , \qquad (2)$$

$$=17.6\times\left(CBR\right)^{0.64} for \ CBR > 5\% , \qquad (3)$$

where CBR is the California Bearing Ratio of subgrade.

The thickness of the binder course in a bituminous pavement may be determined on the basis of radial tensile strain (RTS) (ϵ_t) occurring at the bottom of the bituminous layer at point A or the vertical compressive strain (VCS) (ϵ_v) on the top of subgrade at point B in Fig. 1 at point A and point B, respectively. In bituminous road pavement, radial tensile strain at the bottom of the bituminous layer relates to the pavement performance under fatigue whereas vertical compressive strain on the top of the subgrade relates to the pavement performance under rutting. Modulus and thickness of the unbound granular layer. So, in the present study, the unbound granular layer thickness in a three-layered system has been kept constant for the estimation of binder base thickness. In order to estimate the vertical compressive strain on subgrade or radial tensile strain in asphalt layer due to wheel load using Boussinesq's method [29], the three-layered pavement system needs to be transformed into a homogeneous system by Odemark's approach [29].
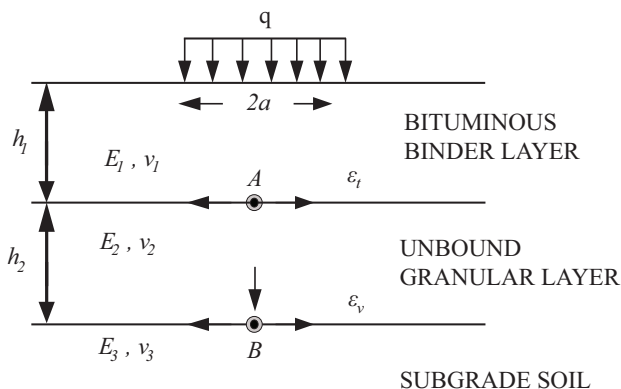

Fig. 1 Typical flexible pavement section in a three-layered system

4 Transformation of multi-layered pavement system to homogeneous system by Odemark's method

Odemark's [29] method assumes that the stress or strain below a layer depends on the stiffness of that layer only. If the thickness, modulus, and Poisson's ratio of layers are changed but the stiffness remains unchanged, the stress and strains below the layer should also remain unchanged. According to Odemark's theory, a two-layered system with different elastic modulus may be transformed into a homogeneous layer as shown in Fig. 2. The two-layer system with the modulus of E_1 with thickness h_1 and Poisson's ratio v_1 as top layer rests on the bottom layer with the modulus of E_2 and the Poisson ratio of v_2, which has been shown in Fig. 2. So, the transformation of such a two-layered system can be done using the concept of the equivalent thickness (h_{eq1}) with an elastic modulus of (E_2), with a Poisson ratio of v_2, in a homogeneous system, which may be expressed as

$$h_{eq1} = f_1 \times h_1 \times \sqrt[3]{\frac{E_1\left(1-v_2^{\ 2}\right)}{E_2\left(1-v_1^{\ 2}\right)}} , \qquad (4)$$

where,

h_{eq1} is termed as equivalent thickness which transforms the two-layered system with elastic modulus E_2 in a homogeneous system in Eq. (4).

f_1 = Odemark's correction factor, which ranges from 0.8 to 1.0 depending on the nature of the respective layer interface under consideration

In the present analysis, if the Poisson's ratio of the layers is considered equal i.e., $v_2 = v_1$ the following relationship may be established from Eq. (4) and has been shown in Eq. (5).

$$h_{eq1} = f_1 \times h_1 \times \sqrt[3]{\frac{E_1}{E_2}} \qquad (5)$$

However, substituting E_2 from Eq. (1) in Eq. (5), Eq. (6) may be developed.

$$h_{eq1} = f_1 \times h_1 \times \sqrt[3]{\frac{E_1}{0.2\times h_2^{\ 0.45}\times E_3}} \qquad (6)$$

The basic principle of transformation of the two-layer system as recommended by Odemark's can further be used to transform a multilayer system into a homogeneous system
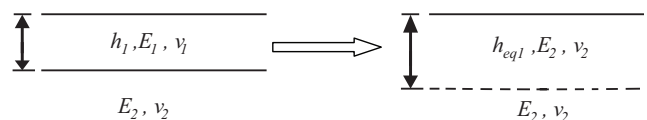

Fig. 2 Transformation of a two-layered system by Odemark's approach

by the successive transformation of different layers. Against this backdrop, a transformation from a three-layered system to a homogeneous system has been made in this paper to apply the standard mechanistic approach of elasticity for the determination of stress, strain, and deflection. The transformation of a three-layer system has been explained in Fig. 3 by a successive transformation of pavement layers starting from binder course to subgrade using Odemark's method. In this analysis, the top two layers with a respective elastic modulus of E_1 and E_2 have primarily been transformed to a homogeneous system with an equivalent thickness of h_{eq1} with an elastic modulus of E_2. Similarly, the transformation of the layer with an elastic modulus of E_2 and E_3 has also been made in this analysis with an equivalent thickness of h_{eq2} with an elastic modulus of E_3.

Therefore,

$$h_{eq2} = f_2 \times \left(h_2 + h_{eq1}\right) \times \sqrt[3]{\frac{E_2}{E_3}} \tag{7}$$

However, substituting E2 from Eq. (1) and heq1 from Eq. (6) in Eq. (7), the following Eq. has been established.

$$h_{eq2} = z_1 = f_2 \times \left(f1 \times h_1 \times \sqrt[3]{\frac{E_1}{0.2 \times h_2^{0.45} \times E_3}} + h_2 \right)$$
$$\times \sqrt[3]{\frac{0.2 \times h_2^{0.45} \times E_3}{E_3}} \tag{8}$$

5 Design of perpetual pavement

In this analytical study, perpetual pavement design has been based on IRC:37-2018 [30], the guideline for the design of flexible road pavement in India. In IRC:37-2018, the pavements with a design load of 300 msa or more have been defined as perpetual pavement which has a minimum age of fifty years. Moreover, according to the guideline, the thickness of the bituminous layer in a three-layered perpetual pavement may be determined on the basis of

an allowable radial tensile strain of 80 $\mu\varepsilon$ at the bottom of a bituminous binder base Similarly, the thickness of a bituminous base may also be obtained by limiting the vertical compressive strain on the top of the subgrade to 200 $\mu\varepsilon$ as recommended in IRC:37-2018. The higher value of the bituminous binder base thus obtained from radial tensile strain and vertical compressive strain has been recommended in this paper as design thickness for perpetual road pavement. Moreover, RTS(ϵ_t) at the bottom of the bitumen layer has been termed as fatigue strain and similarly the VCS(ϵ_v) on top of subgrade as rutting strain.

6 Determination of bituminous layer thickness based on radial tensile strain

According to Boussinesq's theory, in a homogeneous, elastic and isotropic medium with an elastic modulus of E_2, the RTS(ϵ_t) at a depth (z) due to circular load intensity (q) with a contact radius (a) may be expressed as shown in Eq. (9).

$$\epsilon_t = \frac{(1+v) \times q}{2 \times E_2} \left[\frac{-\dfrac{z}{a}}{\left\{ \sqrt{1+\left(\dfrac{z}{a}\right)^2} \right\}^3} - (1-2 \times v) \left\{ \frac{\dfrac{z}{a}}{\sqrt{1+\left(\dfrac{z}{a}\right)^2}} - 1 \right\} \right] \tag{9}$$

However, in order to determine the radial tensile strain at bottom of the bituminous layer in a three-layered pavement, the top two layers have been transformed into a homogeneous system as explained earlier with an equivalent in the present analysis as 450 mm as input parameter which has been adopted for most of the road for sections with relatively higher axle loads as recommended in IRC:37-2018.

In order to determine the radial tensile strain below the bottom of the bituminous layer in the pavement, the top two layers in a three-layered system may be transformed as explained earlier with the equivalent thickness heq1
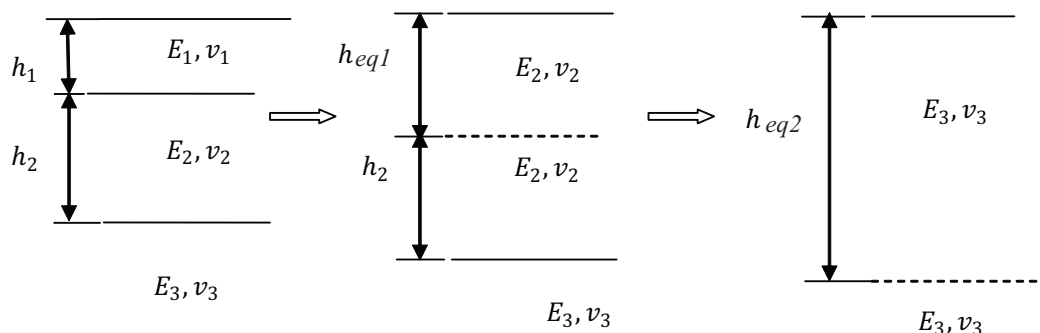

Fig. 3 Successive transformation of a three-layered system by Odemark's approach

as shown in Fig. 4. The Eq. (9) is a generalized equation applicable in a homogeneous system, which has been used in the present analysis by substitution of the term z by transformed depth heq1 as explained in Eq. (6) Assuming $(z/a) = M$, and considering $f = 1.0$ for the layer interface of binder base and unbound granular layer Eq. (6) may further be modified as shown in Eq. (10).

$$\epsilon_t = \frac{(1+v) \times q}{2 \times 0.2 \times h_2^{0.45} \times E_3} \left[\frac{-M}{\left\{ \sqrt{1+(M)^2} \right\}^3} - (1-2 \times v) \left\{ \frac{M}{\sqrt{1+(M)^2}} - 1 \right\} \right]$$

(10)

7 Determination of bituminous binder base thickness based on vertical compressive strain

To determine the vertical compressive strain (ϵ_v) at point B as shown in Fig. 1, the top two layers of the pavement with thickness h_1 and h_2 in a three-layer system have been suitably transformed using Odemark's method as shown in Fig. 3. The vertical compressive strain at point B in an elastic homogeneous medium with an elastic modulus (E_3) at a depth z_1 under circular load intensity (q) at depth z_1 with a contact radius (a) can be obtained using Boussinesq's theory as expressed in Eq. (11).

$$\epsilon_v = \frac{(1+v) \times q}{E_3} \left[\frac{\frac{z_1}{a}}{\left\{ \sqrt{1+\left(\frac{z_1}{a}\right)^2} \right\}^3} - (1-2 \times v) \left\{ \frac{\frac{z_1}{a}}{\sqrt{1+\left(\frac{z_1}{a}\right)^2}} - 1 \right\} \right]$$

(11)

To determine the vertical compressive strain (ϵ_v) at the top of subgrade as shown in Fig. 5, in a three-layered system, the depth (h_{eq2}) up to top of subgrade has been determined in Eq. (8). However, considering $M_2 = z_1/a$ and $f_2 = 0.8$ for the interface of subgrade and unbound granular layer Eq. (11) may further be modified as Eq. (12).
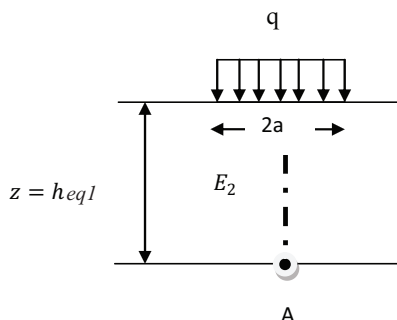
$$\epsilon_v = \frac{(1+v) \times q}{E_3} \left[\frac{M_2}{\left\{ \sqrt{1+(M_2)^2} \right\}^3} - (1-2 \times v) \left\{ \frac{M_2}{\sqrt{1+(M_2)^2}} - 1 \right\} \right]$$

(12)

Therefore, the thickness of the binder base (h_1) in a perpetual pavement may also be estimated by limiting the vertical compressive strain on the top of the subgrade layer. In the present analysis, the allowable strain of 200 $\mu\varepsilon$ has been used in Eq. (12) to estimate the binder base thickness for different subgrade CBR ranging from 5–15%. The higher value of the thickness of binder base obtained from radial tensile strain using Eq. (10) or from vertical compressive strain using Eq. (12) has been considered as design thickness.

8 Design of bituminous binder base thickness based on axle load criteria

An alternative approach for the design of perpetual pavement has been explored in the present paper considering the load-carrying capacity of the pavement as 300 msa as recommended in IRC:37-2018. The allowable radial tensile strain at the bottom of the bituminous layer corresponding to 300 msa load repetitions has been determined from the mechanistic-empirical correlations recommended in IRC:37-2018 and has been shown in Eqs. (13) and (14) for different reliability levels. The allowable strain thus obtained corresponding to 300 msa with 90% reliability level has been used in Eq. (10) for estimation of binder base thickness for different subgrade CBR ranging from 5% to 15%. The allowable fatigue strain in the present analysis for 300 msa load repetitions was obtained corresponding to 300 msa with as 112 $\mu\varepsilon$ considering a 90% reliability level.

$$N_f = 1.6064 \times C \times 10^{-04} \times \left[\frac{1}{\epsilon_t} \right]^{3.89} \times \left[\frac{1}{M_R} \right]^{0.854}$$

(13)

for 80% reliability,

q

2a

$z = h_{eq1}$ E_2

A

Fig. 4 Transformed section up to bottom of binder base
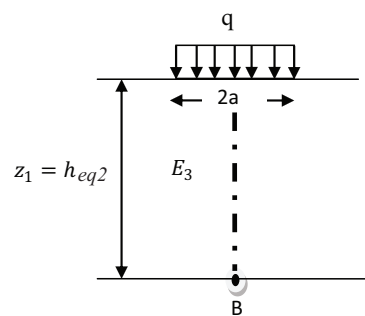
q

2a

$z_1 = h_{eq2}$ E_3

B

Fig. 5 Transformed section up to top of subgrade layer

$$N_f = 0.5161 \times C \times 10^{-04} \times \left[\frac{1}{\epsilon_t}\right]^{3.89} \times \left[\frac{1}{M_R}\right]^{0.854} \tag{14}$$

for 90% reliability,
where $C = 10^M$ and $M = 4.84 \times \left(\dfrac{V_{be}}{V_a + V_{be}} - 0.69\right)$.

N_f = Fatigue life in the number of cumulative standard axles.

ϵ_t = Maximum tensile strain at the bottom of the bituminous layer, and

M_R = Resilient modulus of the bituminous layer. (MPa)

V_{be} = Percent of the volume of effective bitumen in bituminous mix

V_a = Percent of the volume of air voids in bituminous mix

The allowable vertical compressive strain on top of the subgrade has also been determined from the mechanistic-empirical correlations recommended in IRC:37-2018. The correlation between vertical compressive strain and anticipated wheel load repetitions before failure of the pavement under rutting has been expressed in Eq. (15) and Eq. (16) for different reliability levels.

$$N = 4.1656 \times 10^{-08} \times \left[\frac{1}{\epsilon_v}\right]^{4.5337} \tag{15}$$

for 80 % reliability,

$$N = 1.41 \times 10^{-08} \times \left[\frac{1}{\epsilon_v}\right]^{4.5337} \tag{16}$$

for 90 % reliability, where

N = Number of cumulative standard axles before failure in rutting

ϵ_v = Maximum vertical compressive strain on the top of subgrade layer

The allowable vertical compressive strain on the top of the subgrade layer corresponding to 300 msa load repetitions has been obtained as 250 $\mu\varepsilon$ for 300 msa load with 90% reliability level using Eq. (10). The allowable compressive strain thus obtained has been used in Eq. (12) for estimation of binder base thickness for different subgrade CBR ranging from 5% to 15%. It is to be noted that the binder layer thickness has its influence both on radial strain at the bottom of the binder base at the first interface and also on the compressive strain on top of subgrade at the second layer interface, in a three-layered system. Against this backdrop, the design of perpetual pavement in the present paper has been done based on both fatigue and rutting as failure criteria.

9 Input parameters used in pavement design
The input parameters used in the estimation of bituminous binder base thickness are as follows:
- Wheel load = 4100 kg
- Contact pressure of wheel on pavement surface = 0.56 MPa
- Resilient modulus of Bituminous mix = 3000 MPa
- Air voids in bituminous mix = 3.5%
- Volume of effective bitumen in bituminous mix = 11.5%
- Contact radius between tire and pavement = 151 mm
- The combined thickness of unbound granular layer = 450 mm

10 Discussion on test results
The thickness of binder base estimated using present methodology on the basis of allowable fatigue strain of 80 $\mu\varepsilon$ and an allowable rutting strain of 200 $\mu\varepsilon$ have been presented in Table 1 to Table 2. It has been observed that the thickness of the binder base reduces with the increase in subgrade CBR both under fatigue and rutting failure. The thickness of binder base under fatigue was found to vary between 307 mm to 264 mm for change in subgrade CBR from 5% to 15% and the same under rutting was found to range between 308 mm to 203 mm. It is evident from the nature of variation in binder base thickness that the rate of change of thickness is higher under rutting than fatigue. It has been observed in Table 1 and Table 2 that the thickness of the bituminous binder required to

Table 1 Bituminous binder base thickness for perpetual pavement for subgrade CBR from 5–8% based on finite strain criteria

Subgrade CBR (%)	Binder Base thickness against fatigue (mm)	Binder Base thickness against rutting (mm)	Design Thickness of Binder Base (mm)
5	307	309	307
6	301	293	301
7	295	278	295
8	290	265	290

Table 2 Bituminous binder base thickness for perpetual pavement for subgrade CBR from 9–15% based on finite strain criteria

Subgrade CBR (%)	Binder Base thickness against fatigue (mm)	Binder Base thickness against rutting (mm)	Design Thickness of Binder Base (mm)
9	285	255	285
10	281	244	281
12	273	225	273
15	264	203	264

withstand fatigue is generally more than that required to withstand rutting under specified axle load repetitions. Therefore, the recommended thickness for the bituminous binder base has been considered as the thickness obtained against fatigue criteria. Hence, it can be concluded that the performance of perpetual pavement is governed by its failure under fatigue.

Definition of perpetual road pavement includes the load-carrying capacity of road pavement in Indian conditions as 300 msa which may sustain up to 50 years without major distress. Against this backdrop, the bituminous binder base thickness for perpetual pavement has been estimated considering 90% reliability level of fatigue and rutting criteria as mentioned in IRC:37-2018. Therefore, the allowable strain values for perpetual pavement design against rutting as well as fatigue have been determined from Eq. (14) and Eq. (16) corresponding to 300 msa load repetitions. The allowable radial tensile strain and vertical compressive strain were estimated as 112 $\mu\varepsilon$ and 250 $\mu\varepsilon$, respectively, which have been used for the design of binder base using the present methodology. The thicknesses of the binder base thus obtained have been presented in Table 3 and Table 4. It has been observed from the data in Table 3 and Table 4 that, the binder base thickness obtained from fatigue criteria using the present method is higher in comparison to the thickness obtained from rutting criteria. Therefore, the recommended thickness of the binder base shall be governed

by the fatigue strain. The thickness thus obtained based on fatigue strain has been found safe both from cracking and rutting. The thickness of binder base under fatigue was found to vary between 255 mm to 215 mm for change in subgrade CBR from 5% to 15% and the same under rutting was found to vary between 254 mm to 155 mm. It is relevant to mention that the thickness of the binder base of a perpetual road pavement thus obtained considering 300 msa load appears to be less in comparison to the thickness obtained using finite allowable strain under rutting and fatigue. The reason for such reduction in binder base thickness is due to an increase in allowable fatigue strain corresponding to 300 msa load repetitions.

The validation of the present method has been done in this paper by using IITPAVE software. The pavement thickness obtained using the present methodology has been used as an input parameter in IITPAVE software for estimating radial tensile strain at the bottom of the bituminous layer and the vertical compressive strain on the top of the subgrade. The strains thus obtained against fatigue and rutting criteria have been presented in this paper in Table 5. The radial tensile strain obtained from IITPAVE corresponding to binder base thickness estimated using a present methodology based on finite fatigue and rutting strain was in the range between 94 to 91 $\mu\varepsilon$ for subgrade CBR ranging from 5% to 15% whereas the allowable strain of 80 $\mu\varepsilon$ as input parameter was considered for pavement design in the present method. Similarly, the vertical compressive strain obtained from IITPAVE on the top of the subgrade was found to vary between 182 to 141 micro strains. However, for subgrade CBR ranging from 5%

Table 3 Binder base thickness for perpetual pavement for subgrade CBR 5–8% based on finite load criteria

Subgrade CBR (%)	Binder Base thickness against fatigue (mm)	Binder Base thickness against rutting (mm)	Design Thickness of Binder Base (mm)
5	255	254	255
6	250	240	250
7	244	226	244
8	239	213	239

Table 4 Bituminous binder base thickness for perpetual pavement for subgrade CBR 9–15% based on finite load criteria

Subgrade CBR (%)	Binder Base thickness against fatigue (mm)	Binder Base thickness against rutting (mm)	Design Thickness of Binder Base (mm)
9	235	202	235
10	231	193	231
12	224	176	224
15	215	155	215

Table 5 Comparison of binder base thickness using IIT PAVE and present method based on finite strain criteria

Subgrade CBR (%)	Bituminous layer thickness using (Present method) (mm)	Bituminous layer thickness based on IIT PAVE corresponding to 80 $\mu\varepsilon$ fatigue strain (mm)	IITPAVE calculated critical strain	
			Fatigue strain ($\mu\varepsilon$)	Rutting strain ($\mu\varepsilon$)
5	307	340	94	182
6	301	332	93	176
7	295	325	93	170
8	290	320	93	164
9	285	315	93	160
10	281	310	93	156
12	273	300	92	149
15	264	289	91	141

to 15%, the allowable compressive strain of 200 microns was considered as an input parameter for perpetual pavement design in the present method. So, it is evident from the strain data presented in Table 5 that the thickness of the binder base obtained using the present method is quite safe under rutting in terms of IITPAVE output but those fail marginally under fatigue. In this backdrop, the allowable radial tensile strain at the bottom of the bituminous layer may be revised and increased to 95 $\mu\varepsilon$ instead of 80 microns. Similarly, the recommended allowable vertical compressive strain on the top of subgrade may be revised and reduced to 185 $\mu\varepsilon$ instead of 200 $\mu\varepsilon$ considered in the present analysis.

Moreover, the thickness of the binder base for different subgrade CBR has been back-calculated using IITPAVE based on allowable fatigue strain as 80 micro strains and reported in Table 5. It is evident in Table 5 that IITPAVE generated binder base values are 9% more that than the value obtained from the present finite strain-based method and therefore may be considered close and comparable. The range of binder base thickness obtained using the present method was varied from 307 mm to 264 mm for subgrade CBR ranging from 5% to 15%, whereas the thickness of binder base obtained using IITPAVE for the same CBR range varies between 340 mm to 289 mm. The reason for this variation may be explained due to the difference in boundary conditions considered in IITPAVE software and the present analytical method which assumes the failure of pavement as linear and elastic.

The binder base thickness estimated on the basis of 300 msa load repetitions has been used as an input parameter for the determination of fatigue and rutting strain using IITPAVE and presented in Table 6. The thickness of the binder base of pavement obtained using the present method on the basis of allowable fatigue and rutting strain corresponding to 300 msa load has also been reported in this paper.

It is evident from the data presented in Table 6 that the fatigue strain at the bottom of binder base of the pavement sections obtained using the present method varies from 123 $\mu\varepsilon$ to 119 $\mu\varepsilon$ for subgrade CBR ranging from 5% to 15%. Similarly, the rutting strain for the same subgrade CBR was found to vary between 230 $\mu\varepsilon$ to 174 $\mu\varepsilon$. The trend of variation reported in Table 6 shows that the allowable value of fatigue strain and rutting strain may be considered as 120 $\mu\varepsilon$ and 230 $\mu\varepsilon$ respectively, for a perpetual pavement with a design load of 300 msa.

11 Validation of present method using IRC:37-2018

The method proposed in this paper for the estimation of perpetual pavement thickness has been used for the estimation of conventional bituminous road pavement thickness for its validation.

The thickness of binder base of pavement corresponding to specified axle load and subgrade CBR has been determined using the present methodology and those are presented in Table 7 and Table 8 for comparative study. The thickness of the binder base has been obtained in this paper to limit failure of pavement against rutting by solving Eq. (12) and Eq. (16) for different axle load repetitions and subgrade strength. Similarly, the thickness of the binder base has also been determined to limit fatigue failure by solving Eq. (14) and Eq. (10). The higher value of binder base thus obtained against fatigue and rutting has been considered as design thickness.

Table 6 Comparison of binder base thickness using IIT PAVE and present method based on finite axle load

Subgrade CBR (%)	Bituminous layer thickness using (Present method) (mm)	Bituminous layer thickness based on IIT PAVE corresponding to 80 με fatigue strain (mm)	IITPAVE calculated critical strain	
			Fatigue strain (με)	Rutting strain (με)
5	255	272	123	230
6	250	267	123	220
7	244	260	123	213
8	239	255	122	206
9	235	250	121	199
10	231	245	121	194
12	224	236	120	185
15	215	225	119	174

Table 7 Comparison of binder base thickness using present method and IRC-37-2018 for different subgrade CBR and Axle load repetitions

Subgrade CBR (%)	Axle load (5 msa)				Axle load (20 msa)			
	Bituminous Layer thickness using Present Method (mm)				Bituminous Layer thickness using Present Method (mm)			
	IRC:37-2018	Present Method			IRC:37-2018	Present Method		
		Fatigue	Rutting	Design thickness		Fatigue	Rutting	Design \ thickness
5	95.0	99	73	99	145	127	90	127
8	80.0	83	46	83	120	113	59	113
10	80.0	69	31	69	110	105	43	105

Table 8 Comparison of binder base thickness using present method and IRC-37-2018 for different subgrade CBR and Axle load repetitions

Subgrade CBR (%)	Axle load (30 msa)				Axle load (50 msa)			
	Bituminous Layer thickness using Present Method (mm)				Bituminous Layer thickness using Present Method (mm)			
	IRC:37-2018	Present Method			IRC:37-2018	Present Method		
		Fatigue	Rutting	Design thickness		Fatigue	Rutting	Design \ thickness
5	155	164	138	164	180	177	157	177
8	135	151	106	151	155	164	123	164
10	125	143	89	143	145	157	106	157

The thickness of the unbound granular layer in the present analysis has been considered as 450 mm for validation and the subgrade CBR of 5%, 8%, and 10% were considered. The axle load range in the present analysis has been considered between 5-20 msa as lower axle load group and between 30-50 msa as higher axle load group. The design thickness of the binder base thus obtained using the present method has been compared with relevant layer thickness recommended in IRC:37-2018 in Table 7 and Table 8. It is evident from the data presented in Table 7 and Table 8 that the binder base thickness obtained using the present method is reasonably close with respect to the binder base thickness recommended in IRC:37-2018 for low to high CBR and also for low to high axle load groups.

It may be noted that, for a lower axle load of 5 msa with subgrade CBR 5% and 8%, the variation in binder base thickness obtained by two different methods were in between 4.2% and 3.7%, respectively.

However, for a higher axle load of 50 msa, the same variation in binder base for subgrade CBR 5% and 8% were found to 1.8% and 5.1% respectively. It has been found that the variation in binder base thickness between the two methods is marginal for higher subgrade CBR with higher axle loads. In this backdrop, the observed convergence of binder base data justifies the acceptability of present method.

12 Conclusions

The methodology for perpetual pavement design proposed in this study can further be used for the estimation of conventional bituminous pavement thickness considering the pavement as a multi-layered system. The reliability of the method has been compared with IRC:37-2018 and found to be satisfactory. It has been observed in the present analysis that the thickness of the binder base required to withstand fatigue is generally more than that required to withstand rutting under a specified axle load repetition. Therefore, it can be concluded that the performance of perpetual pavement is governed by its failure under fatigue.

It is relevant to mention that the thickness of the binder base in a perpetual road pavement obtained using 300 msa load appears to be less than the thickness obtained using finite strain-based criteria. For validation of the present method, fatigue and rutting strains were estimated using IITPAVE for the pavement thickness obtained using the present methodology. It has been found from the critical strain values, that the allowable radial tensile strain at the bottom of a bituminous layer may be revised as 95 $\mu\varepsilon$ instead of 80 $\mu\varepsilon$ as recommended in IRC:37-2018. Moreover, the allowable vertical compressive strain on the top of the subgrade may also be modified and reduced to 185 $\mu\varepsilon$ instead of 200 $\mu\varepsilon$ considered. However, the allowable fatigue or rutting strains for the design of perpetual road pavement may increase if the design load of 300 msa is considered. Moreover, the thickness of the binder base obtained using IITPAVE and the present study shows good convergence. Therefore, the present method of pavement design may be considered as an alternative and reliable approach.

References

[1] Robbins, M. M., Tran, N. H., Timm, D. H., Willis, J. R. "Adaptation and validation of stochastic limiting strain distribution and fatigue ratio concepts for perpetual pavement design", Road Materials and Pavement Design, 16(S2), pp. 100–124, 2015.
http://doi.org/10.1080/14680629.2015.1077001

[2] Beriha, B., Sahoo, U. C., Steyn, W. J. "Determination of endurance limit for different bound materials used in pavements: A review", International Journal of Transportation Science and Technology, 8(3), pp. 263–279, 2019.
https://doi.org/10.1016/j.ijtst.2019.05.002

[3] Nunn, M. E., Brown, A., Weston, D., Nicholls, J. C. "Design of Long-Life Flexible Pavements for Heavy Traffic", Transportation Research Laboratory, Berkshire, UK, TRL Report No. 250, 1997.

[4] Cao, W., Norouzi, A., Kim, Y. R. "Application of viscoelastic continuum damage approach to predict fatigue performance of Binzhou perpetual pavements", Journal of Traffic and Transportation Engineering, 3(2), pp. 104–115, 2016.
https://doi.org/10.1016/j.jtte.2016.03.002

[5] Newcomb, D. E., Buncher, M., Huddleston, I. J. "Concepts of Perpetual Pavements", Transportation Research Circular, 503, pp. 4–11, 2001.

[6] Sidess, A., Uzan, J. "A design method of perpetual flexible pavement in Israel", International Journal of Pavement Engineering, 10(4), pp. 241–249, 2009.
http://doi.org/10.1080/10298430701830225

[7] Yang, Y., Gao, X., Lin, W., Timm, D. H., Priest, A. L., Huber, G. A., Andrewski, D. A. "Perpetual pavement design in China", presented at: International Conference on Perpetual Pavements, Columbus, OH, USA, Szept. 13–14, 2006.

[8] Newcomb, D. E., Willis, R., Timm, D. H. "Perpetual Asphalt Pavements: A Synthesis", Asphalt Pavement Association of Michigan, Okemos, MI, USA, IM-40, 2010.

[9] Khiavi, A. K., Ameri, M. "Laboratory evaluation of strain-controlled fatigue criteria in hot mix asphalt", Construction and Building Materials, 47, pp. 1497–1502, 2013.
https://doi.org/10.1016/j.conbuildmat.2013.06.062

[10] Thompson, M. R, Carpenter, S. H. "Considering hot mix asphalt fatigue endurance limit in full depth mechanistic-empirical pavement design", University of Illinois Urbana-Champaign, Urbana, IL, USA, 2006.

[11] Monismith, C.L., McLean, D.B. "Structural design considerations", Association of Asphalt Paving Technologists, 41, pp. 258–304, 1972.

[12] Prowell, B. D., Brown, E. R., Andesron R. M., Daniel, J. S., Swamy, A. K., Von Quintus, H., Shen, S., Carpenter, S. H., Bhattacharjee, S., Maghsoodloo, S. "Validating the fatigue endurance limit for asphalt pavements", Transportation Research Board, Washington, DC, USA, 2010.
https://doi.org/10.17226/14360

[13] Carpenter, S. H., Shen, S. "Dissipated Energy Approach to Study Hot-Mix Asphalt Healing in Fatigue", Transportation Research Record, 1970(1), pp. 178–185, 2006.
http://doi.org/10.1177/0361198106197000119

[14] Sabouri, M. "An investigation on perpetual asphalt pavements in Minnesota", International Journal of Pavement Research and Technology, 13, pp. 247–254, 2020.
https://doi.org/10.1007/s42947-020-0149-2

[15] Sakhaeifar, M. S., Brown, E. R., Tran, N., Dean, J. "Evaluation of Long-Lasting Perpetual Asphalt Pavement with Life-Cycle Cost Analysis", Transportation Research Record, 2368, pp. 3–11, 2013.
https://doi.org/10.3141/2368-01

[16] Timm, D. H., Newcomb, D. E, Immanuel, S. S. "A Practical Guide to Low Volume Road Perpetual Pavement Design", presented at: International Conference on Perpetual Pavements, Columbus, OH, USA, Szept. 13–14, 2006.

[17] Lee, S. I., Carrasco, G., Mahmoud, E., Walubita, L. F. "Alternative Structure and Material Designs for Cost-Effective Perpetual Pavements in Texas", Journal of Transportation Engineering, Part B: Pavements, 146(4), 04020071, 2020.
https://doi.org/10.1061/JPEODX.0000226

[18] Priyanka, B. A, Sarang, G., Shankar, A. U. R. "Evaluation of Superpave mixtures for perpetual asphalt pavements", Road Materials and Pavement Design, 20(8), pp. 1952–1965, 2019.
https://doi.org/10.1080/14680629.2018.1474794

[19] Qadir, A., Gazder, U., Ali, S. "Comparison of SBS and PP fiber asphalt modifications for rutting potential and life cycle costs of flexible pavements", Road Materials and Pavement Design, 19(2), pp. 484–493, 2018.
https://doi.org/10.1080/14680629.2016.1259124

[20] Islam, S., Sufian, A., Hossain, M., Miller, R, Leibrock, C. "Mechanistic-Empirical design of perpetual pavement", Road Materials and Pavement Design, 21(5), pp. 1224–1237, 2020.
http://doi.org/10.1080/14680629.2018.1546218

[21] Kollaros, G., Athanasopoulou, A., Kokkalis, A. "Perpetual flexible pavement design life", In: Proceedings of the 10th International Conference on the Bearing Capacity of Roads, Railways and Airfields (BCRRA 2017), Athens, Greece, 2017, pp. 537–542.

[22] Scheer, M. J. "Impact of Pavement Thickness on Load Response of Perpetual Pavement", MsC Thesis, Ohio University, 2013. [online] Available at: http://rave.ohiolink.edu/etdc/view?acc_num=ohiou1371636949

[23] Das, A. "Structural Design of Asphalt Pavements: Principles and Practices in Various Design Guidelines", Transportation in Developing Economies, 1, pp. 25–32, 2015.
https://doi.org/10.1007/s40890-015-0004-3

[24] Mazumder, M., Kim, H., Lee, S.-J. "Perpetual pavement: future pavement network", Journal of Advanced Construction Materials, 19(1), pp. 35–49, 2015.

[25] Liao, J., Sargand, S. "Viscoelastic FE Modeling and Verification of a U.S. 30 Perpetual Pavement Test Section", Road Materials and Pavement Design, 11(4), pp. 993–1008, 2010.
http://doi.org/10.1080/14680629.2010.9690316

[26] Romanoschi, S. A., Gisi, A. J., Portillo, M., Dumitru, C. "First Findings from the Kansas Perpetual Pavements Experiment", Transportation Research Record: Journal of the Transportation Research Board, 2068(1), pp. 41–48, 2008.
http://doi.org/10.3141/2068-05

[27] Kulkarni, S., Ranadive, M. "Effect of Change in the Resilient Modulus of Bituminous Mix on the Design of Flexible Perpetual Pavement", In: Pawar P. M., Balasubramaniam R., Ronge B. P., Salunkhe S. B., Vibhute A. S., Melinamath B. (eds.) Techno-Societal 2020, Springer, 2020, pp. 829–839.
https://doi.org/10.1007/978-3-030-69921-5_83

[28] Powell, W. D., Potter, J. F., Mayhew, H. C., Nunn, M. E. "The Structural Design of Bituminous Roads", Pavement Design and Maintenance Division Highways and Structures Department Transport and Road Research Laboratory, Crowthorne, Berkshire, UK, TRRL Lab. Report1132, 1984.

[29] Odemark "Investigations as to the elastic properties of soils and design of pavements according to the theory of elasticity", Statens Vaginstitut, Stockholm, Sweden, 1949. [in Swedish] ˙(online) Available at: urn:nbn:se:vti:diva-8079

[30] Indian Roads Congress "Guidelines for the design of flexible pavements", Indian Roads Congress, New Delhi, India, Rep. IRC:37-2018, 2018.